

Structures of mixed argon-nitrogen clusters

Masanari Nagasaka, Ertugrul Serdaroglu, Roman Flesch, Eckart Rühl, and Nobuhiro Kosugi

Citation: *The Journal of Chemical Physics* **137**, 214305 (2012); doi: 10.1063/1.4768423

View online: <http://dx.doi.org/10.1063/1.4768423>

View Table of Contents: <http://scitation.aip.org/content/aip/journal/jcp/137/21?ver=pdfcov>

Published by the [AIP Publishing](#)

Articles you may be interested in

[A path-integral Monte Carlo study of a small cluster: The Ar trimer](#)

J. Chem. Phys. **132**, 244303 (2010); 10.1063/1.3445773

[Hybrid diatomics-in-molecules-based quantum mechanical/molecular mechanical approach applied to the modeling of structures and spectra of mixed molecular clusters Ar_n \(HCl\)_m and Ar_n \(HF\)_m](#)

J. Chem. Phys. **120**, 3732 (2004); 10.1063/1.1642596

[Structural motifs and stability of small argon–nitrogen clusters](#)

J. Chem. Phys. **119**, 9021 (2003); 10.1063/1.1614751

[Structure and charge transfer dynamics of the \(Ar–N₂\)⁺ molecular cluster](#)

J. Chem. Phys. **115**, 8888 (2001); 10.1063/1.1413980

[Homogeneous and mixed UF₆ clusters with Ar: Calculations of structures and vibrational spectra](#)

J. Chem. Phys. **109**, 8295 (1998); 10.1063/1.477492



AIP | APL Photonics

APL Photonics is pleased to announce
Benjamin Eggleton as its Editor-in-Chief



Structures of mixed argon-nitrogen clusters

Masanari Nagasaka,^{1,2,a)} Ertugrul Serdaroglu,³ Roman Flesch,³ Eckart Rühl,³
and Nobuhiro Kosugi^{1,2}

¹*Institute for Molecular Science, Myodaiji, Okazaki 444-8585, Japan*

²*The Graduate University for Advanced Studies, Myodaiji, Okazaki 444-8585, Japan*

³*Physikalische Chemie, Freie Universität Berlin, Takustr. 3, D-14195 Berlin, Germany*

(Received 14 July 2012; accepted 7 November 2012; published online 4 December 2012)

The structures of mixed argon-nitrogen clusters of different compositions are investigated by analyzing core level shifts and relative intensities of surface and bulk sites in the Ar $2p_{3/2}$ regime in soft X-ray photoelectron spectroscopy. These structures are confirmed by core level shift calculations taking induced dipole interactions into account, in which several model structures of the mixed clusters are considered by Monte Carlo simulations. These results suggest that the mixed argon-nitrogen clusters show partial core-shell structures, where an argon core is partially covered by nitrogen molecules.

© 2012 American Institute of Physics. [<http://dx.doi.org/10.1063/1.4768423>]

I. INTRODUCTION

Structures of rare gas clusters formed by van der Waals interactions¹ are widely investigated by element-selective core-level excitations and ionizations.² Most rare gas clusters with more than 10^3 atoms are found in face-centered-cubic (fcc) crystalline structure. Surface and bulk sites of the clusters are clearly distinguished by core level shifts in soft X-ray photoelectron spectroscopy (XPS).³ Small clusters containing less than 200 atoms are mostly found in icosahedral structures, in which the surface of the cluster is not close packed.⁴ Recently, we investigated changes in surface structures of small Kr clusters with an average size up to 30 atoms per cluster by using XPS.⁵ Different core level shifts were assigned to different surface sites of the clusters. These energy shifts are caused by induction or polarization of atoms surrounding the absorbing site and are induced by the singly charged ion which is formed by the photoionization process.^{6,7} The surface sites of clusters have also been distinguished by exchange interactions of Rydberg electrons with the surrounding atoms by recent X-ray absorption^{8,9} and resonant Auger electron¹⁰ studies.

Mixed rare gas clusters are formed either by doping pre-made rare gas clusters by another species^{11–14} or by co-expansion of two different species.^{15–20} It is discussed that mixed rare gas clusters formed by the doping method show thermodynamically less stable structures than those obtained from coexpansion of the constituents. Mixed rare gas clusters formed by coexpansion in the size regime of about 10^3 atoms per cluster were investigated by using XPS.^{15–18} Because of the large size of the clusters, their surface energy is not a dominant factor. On the other hand, the structures of small mixed clusters are influenced by several factors, where not only the inter-atomic interaction energies but also the surface energies and the atomic radii play a role. Clarke *et al.*

have performed Monte Carlo simulations on mixed rare gas clusters by changing the inter-atomic interaction energies in the Lennard-Jones potentials.²¹ From this work, they revealed the structural phase diagram of mixed clusters with different inter-atomic interaction energies. Nagaya *et al.* measured Kr K-edge X-ray absorption spectra of small mixed Ar-Kr clusters with low Kr concentrations.¹⁹ They found that these mixed clusters consist of core-shell structures. Recently, we investigated the structures of small mixed Kr-Xe clusters with an average size of 30–37 atoms per cluster by using XPS.²⁰ We revealed that small Xe cores are partly embedded on the surface of Kr clusters. These Xe cores may grow and merge leading to a phase separation between both rare gas moieties with increasing the Xe content. Such phase separation has also been deduced from Monte Carlo simulations.²²

The inter-atomic potential of rare gas atom is isotropic. In contrast, diatomic molecules show anisotropic potentials as a result of the molecular geometry. Several groups investigated the structures of mixed molecular clusters before.^{23–31} Earlier, the structures of rare gas clusters mixed with SF₆ were investigated.^{32–36} Mixed argon-nitrogen clusters are easily formed due to the small difference in inter-molecular potentials.^{37,38} The structure and electronic properties of mixed Ar-N₂ clusters were investigated by electron diffraction,³⁹ surface scattering,⁴⁰ X-ray absorption spectroscopy, and zero kinetic energy photoelectron spectroscopy.⁴¹ These studies suggested that the mixed argon-nitrogen clusters show core-shell structures, in which Ar atoms form a core covered by nitrogen molecules. However, the structural details of mixed Ar-N₂ clusters have not been fully understood.

In the present work, we investigate the structures of the small mixed Ar-N₂ clusters of different compositions by using XPS. The mixed clusters are produced by coexpansion of the gas mixtures by varying the mixing ratio of both gases. Core level shifts and relative intensities of the surface and bulk sites are analyzed in Ar $2p_{3/2}$ XPS spectra with the help of Monte Carlo simulations and core level shift calculations.

^{a)}Electronic mail: nagasaka@ims.ac.jp.

II. METHODS

A. Experiments

The XPS measurements on mixed Ar-N₂ clusters were performed at the soft X-ray in-vacuum undulator beamline BL3U at the storage ring UVSOR-II.⁴² The excitation energy was set to 302 eV to probe the Ar 2*p*_{3/2} regime. This yields a kinetic energy of the photoelectron of about 50 eV, since the 2*p*_{3/2} binding energy of Ar atom is 248.629 ± 0.010 eV.⁴³ The present XPS may be surface sensitive considering a small attenuation length of ~50 eV kinetic energy electrons.⁴⁴ The XPS spectra were measured by using a hemispherical electron energy analyzer (SCIENIA SES-200 combined with a MBS A-1 control system). The analyzer is mounted at ~55° to the horizontal polarization plane of the synchrotron radiation (magic angle) to avoid the angular distribution effect of electron emission.⁴⁵ The pass energy was set to 50 eV, and the bandwidth of the incident photons was set to 200 meV, yielding a total energy resolution ~225 meV. The cluster peaks in XPS spectra were observed at the lower binding energy of the atomic signals, similar to earlier work.^{3,5} The Ar atomic peaks in XPS spectra were fitted by Voigt profiles, in which the effective Gaussian contribution is 251 meV and the Lorentzian width is 118 meV, considering the core-hole life time.⁴⁶ Although X-ray absorption spectroscopy near the nitrogen K-edge of nitrogen clusters was previously reported,^{47,48} N 1*s* XPS measurements were difficult using the present experimental setup since the photon flux at the N 1*s* region in the beamline BL3U is lower than that at the Ar 2*p* region and it is not sufficient to measure XPS spectra of small mixed Ar-N₂ clusters. Valence photoelectron spectroscopy is an effective method to observe the contributions of both Ar and N₂ in the mixed clusters, but it is generally difficult to distinguish the surface and bulk sites.⁴⁹ Therefore, we focus on the core-level photoelectron spectroscopy in the present work.

Mixed Ar-N₂ clusters were formed in a supersonic gas expansion of the primary gas mixtures. The detailed experimental setup has been described previously.^{5,20} The gas mixtures containing 10–40 at. % Ar was controlled by a real time gas mixing apparatus (GB-2C, Kofloc Co., Ltd.). The gas mixture was expanded through a 50 μm nozzle into the vacuum with a stagnation pressure of 0.5 MPa at a temperature of 163 K. The average cluster size of homogeneous Ar clusters was estimated to be 200 atoms per cluster considering the expansion conditions and the correlation with the average cluster size proposed by Karnbach *et al.*⁵⁰ The fraction of Ar atoms in the mixed clusters is evaluated from the Ar 2*p*_{3/2} XPS-intensities in comparison with that of the homogeneous Ar clusters with an average size of 200 atoms per cluster. The average number of Ar surface and bulk sites is obtained from the different binding energy shifts of the cluster peaks because the binding energy shift reflects the size of the cluster (cf., e.g., Ref. 5). The average size of nitrogen clusters in the jet is estimated from the expansion conditions, as based on earlier work (cf. Refs. 24, 47, 48, and 51). Note that only the partial stagnation pressure of nitrogen in the gas mixture is used for this estimate. The expansion condition would lead in neat expansions of the Ar and N₂ components to massive cluster formations. Then, the estimated quantity of N₂

molecules in mixed clusters might be different from the true value. However, in a Ar/N₂-gas mixture, both the components can act under the applied expansion condition as a seed for further growth of mixed clusters. Therefore, any corrections of the above mentioned assumptions to estimate the average cluster size appear to be arbitrary. As a result in the present work, the average composition of the mixed clusters is determined by a summation of both individually determined sizes of the constituents. The average size of the mixed clusters formed from the 10, 20, and 40 at. % Ar mixtures are evaluated to be Ar₂₈(N₂)₄₈ (37% Ar), Ar₆₂(N₂)₃₁ (67% Ar), and Ar₁₃₆(N₂)₁₁ (97% Ar), respectively. The cluster size estimation is not only based on the peak intensity analysis but also on the site-dependent peak shift analysis. A similar discussion on the cluster peak shift has been recently reported.⁵² A previous surface scattering study revealed that the gas mixture containing 9 at. % Ar yields 35% argon in the mixed Ar-N₂ clusters.⁴⁰ This result is consistent with the present estimate on the composition of the mixed clusters.

B. Theoretical simulations

The core level shifts of the surface and bulk sites in several structural models of mixed Ar-N₂ clusters were derived by taking the induced polarization into account. Several model structures of the clusters were optimized by Monte Carlo simulations (cf. Ref. 20).

The potentials of Ar-Ar, Ar-N₂, and N₂-N₂ pairs were referred from previous work of Hewage *et al.*^{37,38} The interaction of the Ar-Ar pair was described by the HFD-C potential proposed by Aziz and Chen.⁵³ The well depth and the equilibrium distance of the potential are 143.22 K and 3.76 Å, respectively. The interaction of the Ar-N₂ pair was proposed by Bowers, Tang, and Toennies.⁵⁴ The radial potentials at three different angles (0°, 45°, and 90°) between the N₂ bond vector and the dimer axis were described by Born-Mayer and dispersion terms. The potential at any other angle was obtained from Legendre polynomial interpolation of the three radial potentials. The potential at an angle of 90° is most stable, in which the well depth and the equilibrium distance are 160.91 K and 3.65 Å, respectively. The interaction of the N₂-N₂ pair was determined by Böhm and Ahlrichs.⁵⁵ The N₂ molecule is treated as a rigid rotor, and the potential is described in terms of four coordinate variables as the molecular distance, the polar angles of the two molecules relative to the dimer axis, and the azimuthal angle between both molecules. The potential consists of a Buckingham term describing the repulsion between the molecules and the electronic potential of the quadrupole moment. The N₂-N₂ pair shows two stable structures: (i) a T-shaped structure, where one N₂ bond vector is perpendicular to the other one, and (ii) a canted parallel structure where two N₂ bond vectors are parallel to each other with a tilt angle of 57°. The well depth and equilibrium distance of the T-shaped structure are 148.00 K and 4.15 Å, whereas the parameters of the canted parallel structure are 147.40 K and 3.98 Å, respectively.

The Ar clusters were optimized from randomly distributed atoms at 100 K by cooling these gradually to 0 K

by using the Metropolis method.⁵⁶ The aim of the present simulations is a comparison of typical model structures in order to simulate the experimental results, rather than the complete optimization of the global minimum of cluster structures. This appears to be reasonable, since it is known that kinetically controlled defect structures are often formed in jet expansions.^{4,5} Finally, for initial geometries of mixed Ar-N₂ clusters, we used the optimized structures of argon clusters at 0 K and replaced some of the Ar atoms by N₂, so that the experimentally estimated mixing ratio of both moieties was reached. After replacing some of the Ar atoms, the mixed cluster structures were relaxed at T = 0 K in order to reach the appropriate inter-molecular distances in the mixed clusters. Note that both the position and orientation of the nitrogen molecule is optimized by using the potentials of the Ar-N₂ and N₂-N₂ pairs.^{54,55} These optimized structures do not consider the thermal excitation, which is contained in the jet expansion. This seems to be justified, since we are only modeling reasonable structural motives.

The core level shifts at the surface and bulk sites in mixed Ar-N₂ clusters from the isolated Ar atom were determined by using energy shift calculations considering induced dipole polarizations.^{6,7} This method was also applied to the molecular clusters.^{31,57-59} The molecule *i* near an ionized atom has the induced dipole moment $\mathbf{p}_i = \alpha_i \mathbf{E}_i$. The polarizability α of Ar is 1.64 Å³.⁶⁰ The polarizabilities of N₂ along the molecular and the perpendicular axes are 2.38 Å³ and 1.45 Å³, respectively.⁶¹ The electric field vector $E_{i,\mu}$ of the molecule *i* is described by

$$E_{i,\mu} = E_{i,\mu}^0 - \frac{1}{4\pi\epsilon_0} \sum_{j \neq i} \sum_v^3 M_{\mu\nu}(\mathbf{r}_i - \mathbf{r}_j) p_{j,\nu}. \quad (1)$$

The first term in Eq. (1) is the initial electric field caused by the Coulomb interaction of the singly charged ion and by the quadrupole moments of the N₂ molecules. Note that the interaction of the quadrupole moment of the N₂ molecule is at the same level as the induced dipole-dipole interactions. The second term is the electric field of the induced dipole moments from surrounding molecules *j*. The tensor $M_{\mu\nu}(\mathbf{R})$ is described by $M_{\mu\nu}(\mathbf{R}) = (\delta_{\mu,\nu} R^2 - 3R_\mu R_\nu)/R^5$. Since $E_{i,\mu}$ includes the contribution from different molecules *j*, the solution should be obtained self-consistently. The core level shift S_a at the singly charged ion *a* is obtained from the sum of the induced dipole moments and the initial electric field as

$$S_a = -\frac{1}{2} \sum_i^N \mathbf{p}_i \cdot \mathbf{E}_i^0. \quad (2)$$

Although the initial state of the cluster is shifted from the isolated atom due to the induced dipole moments caused by the quadrupole moment of the nitrogen molecule, we have confirmed this energy shift is too small (within -0.001 eV) to affect the calculated core level shifts. Finally, we summed up the contributions of all Ar atoms *a* in the cluster to derive the simulated spectra after convolution by a Gaussian profile with a width of 0.3 eV. The number of the nearest neighbors at the bulk sites is expected to be 12, where the other species correspond to various surface sites with slightly dif-

ferent coordination numbers ranging between 6 and 9 for perfect icosahedra.⁶²

III. RESULTS AND DISCUSSION

A. Core level shift analysis of experimental spectra

Figure 1 shows the Ar 2p_{3/2} XPS spectra of the mixed Ar-N₂ clusters with different compositions, as derived from the approach outlined in Sec. II A. The cluster peaks show a lower binding energy compared to the atomic peak. They are blended and can be de-convoluted by the fitting procedures using Voigt profiles, as described in Sec. II A. This allows us to distinguish surface and bulk sites of the clusters, where the lowest binding energy is observed for the bulk sites, similar to the earlier work.^{3,5} The binding energies and the relative intensities of the surface and bulk sites are compiled in Table I. We have estimated that the signal-to-noise ratio is about 10% in the XPS spectra of the mixed Ar₂₈(N₂)₄₈ clusters (37% Ar). Considering that the average composition of Ar in mixed clusters is 28 atoms, leads to an error limit of ±3 Ar atoms. The error in the binding energy shift is estimated to be within 0.03 eV.

In Ar₂₀₀ (100% Ar), the surface and bulk sites show a shift to lower binding energy by 0.62 eV and 0.90 eV relative to the atomic signal, respectively. The intensity ratio of the surface and bulk sites is used to estimate the average number of surface and bulk sites, yielding 124 surface sites and 76 bulk sites, respectively. This estimate is reasonable, considering that small clusters with a size of 200 atoms have ~120 surface atoms (115 for icosahedral or cuboctahedral fcc structures). Therefore, in the present work, the photoelectrons

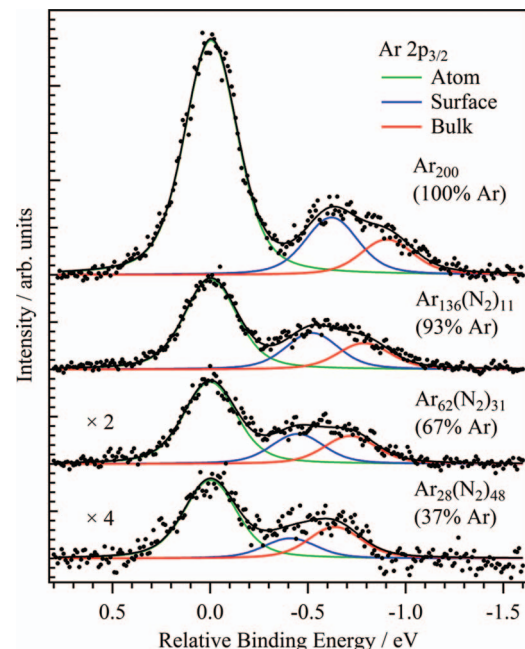


FIG. 1. Ar 2p_{3/2} XPS spectra of mixed Ar-N₂ clusters. The average fraction of Ar is shown in parentheses. The horizontal axis is the relative binding energy from atomic argon. The contributions of Ar atoms as well as Ar surface and bulk sites in mixed clusters are derived from a fitting procedure (see text for further details).

TABLE I. Experimental and calculated Ar $2p_{3/2}$ binding energy shifts (in eV) of surface and bulk sites in mixed Ar-N₂ clusters relative to the atomic peak. The estimated average fraction of Ar atoms is indicated in parentheses in column 1. The numbers of Ar atoms at surface and bulk sites of the clusters is indicated in parentheses of columns 2 and 3.

Composition	Binding energy shift (eV)	
	Surface	Bulk
Experiments		
Ar ₂₀₀ (100% Ar)	-0.62 (124)	-0.90 (76)
Ar ₁₃₆ (N ₂) ₁₁ (93% Ar)	-0.52 (79)	-0.79 (57)
Ar ₆₂ (N ₂) ₃₁ (67% Ar)	-0.45 (32)	-0.72 (30)
Ar ₂₈ (N ₂) ₄₈ (37% Ar)	-0.41 (11)	-0.64 (17)
Calculations		
Ar ₂₀₀ (100% Ar)	-0.58 (122)	-0.90 (78)
Ar ₁₃₆ (N ₂) ₁₁ (93% Ar)	-0.56 (80)	-0.87 (56)
Ar ₆₂ (N ₂) ₃₁ (67% Ar)	-0.53 (34)	-0.82 (28)
Ar ₂₈ (N ₂) ₄₈ (37% Ar)		
Model A	-0.51 (22)	-0.79 (6)
Model B	-0.50 (20)	-0.77 (8)
Model C	-0.71 (10)	-0.78 (18)
Model D	-0.54 (11)	-0.78 (17)

with ~ 50 eV kinetic energies emitted from the bulk sites of ~ 200 atoms do not seem to be influenced significantly by the small escape depth, namely, the intensity suppression caused by the inelastic scattering.⁴⁴

In mixed Ar-N₂ clusters, the binding energy shifts of both the surface and bulk sites become smaller with decreasing the Ar mixing ratio. The intensity of the Ar surface sites also decreases in comparison with that of the Ar bulk sites. In the Ar₂₈(N₂)₄₈ clusters (37% Ar), the binding energy shifts of the surface and bulk sites are 0.41 eV and 0.64 eV, respectively. The average number of Ar atoms in the surface sites is 11, and is smaller than that of the bulk sites (17 atoms). The decrease of the Ar surface sites is rationalized by the fact that the argon is covered by nitrogen. This is consistent with earlier findings obtained from photoion yields of mixed clusters.⁴¹ The polarizability of nitrogen molecule at the molecular axis (2.38 \AA^3)⁶¹ is larger than that of argon (1.64 \AA^3),⁶⁰ but the polarizability of nitrogen at the perpendicular axis (1.45 \AA^3)⁶¹ is smaller than that of the argon atom. The smaller binding energy shifts of the Ar bulk sites would imply that nitrogen molecules occupy the surface in mixed clusters, which are perpendicularly oriented relative to the argon atoms. This is consistent with the potential of the Ar-N₂ dimer, in which the most stable structure is the perpendicular orientation of the N₂ bond vector relative to the dimer axis.⁵⁴ The reduction in size of the mixed clusters also affects the smaller binding energy shifts of the Ar bulk sites. The relations between the energy shifts and the structures of the mixed clusters are discussed in Sec. III B. The binding energy shifts of the surface sites in mixed clusters are also important for investigating their structures. The energy shifts of the surface sites are discussed in comparison to results from calculation shown in Sec. III B. If the Ar core is covered by N₂ in Ar₂₈(N₂)₄₈ clusters (37% Ar), the statistical average number of argon occupying surface sites is estimated to be 12. This estimate is close to the

experimental result, where 11 argon sites are derived to be on the surface. The intensity ratios of the surface and bulk sites in Ar₆₂(N₂)₃₁ (67% Ar) and Ar₁₃₆(N₂)₁₁ (93% Ar) can be analyzed in a similar way. This also leads to the conclusion that these clusters also show the core-shell structures, in which Ar atoms preferably occupy the bulk sites and are covered by nitrogen molecules.

B. Comparison with model calculations

In order to compare the experimentally proposed structures of mixed Ar-N₂ clusters with plausible model structures, the binding energies and intensities of the XPS spectra were simulated by the theoretical approach outlined in Sec. II B. Figure 2 shows simulated Ar $2p_{3/2}$ XPS spectra for four different model structures of Ar₂₈(N₂)₄₈ (37% Ar). The binding energy shifts and the intensities of the surface and bulk sites in the different models of the mixed clusters are enlisted in Table I. The number of Ar atoms at surface and bulk sites of Ar₂₀₀ is 122 and 78, respectively. This is consistent with the experimental results. In the case of mixed clusters, we considered first model A for Ar₂₈(N₂)₄₈ clusters (37% Ar), in which the Ar atoms and N₂ molecules are randomly distributed. Note that both the position and orientation of the nitrogen molecule are optimized by using the potentials of the Ar-N₂ and N₂-N₂ pairs.^{54,55} Clearly, the number of bulk sites

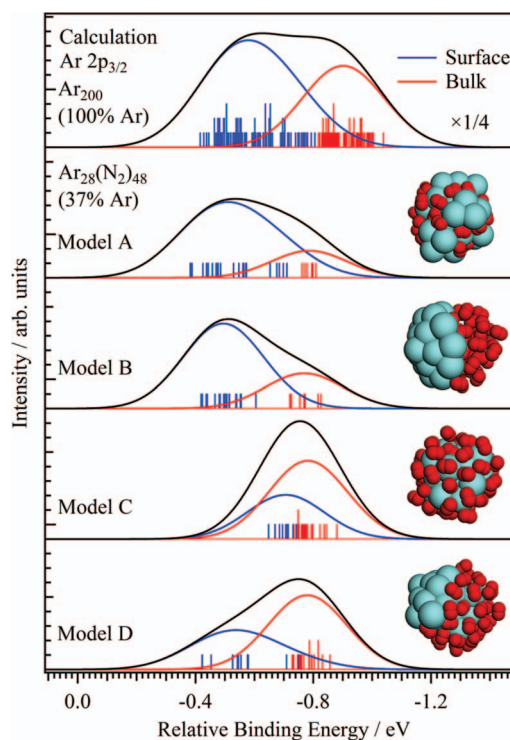


FIG. 2. Calculated Ar $2p_{3/2}$ binding energies (relative to the atomic values) and intensities of the surface and bulk sites in four different model structures of the Ar₂₈(N₂)₄₈ clusters (37% Ar), in comparison with the Ar₂₀₀ cluster. Simulated model structures of the mixed clusters are shown, in which Ar and N atoms are indicated by green and red spheres, respectively. Each vertical bar corresponds to the core level shift of different Ar sites in clusters. These are broadened by Gaussian line shapes (see text for further details). The total energy of models B, C, and D relative to model A are +0.07 eV, -0.20 eV, and -0.12 eV, respectively.

is smaller than that of surface sites in icosahedral structures. Therefore, the intensity of the bulk sites is lower than that of the surface sites. However, this intensity ratio is quite inconsistent with the experimental results. In model B, a phase separation between Ar and N₂ has occurred in mixed clusters. Note that our recent experimental work on small mixed Kr-Xe cluster shows such phase separation behavior.²⁰ However, for argon-nitrogen mixtures the intensity ratio of the surface and bulk sites is also inconsistent with the experimental XPS spectrum (see Fig. 1). Clarke *et al.* proposed a phase diagram of mixed atomic clusters.²¹ This phase diagram relates the interaction energy of atoms and the structures of mixed clusters. Although mixed argon-nitrogen clusters are not atomic clusters, it is interesting to discuss the structures of the mixed argon-nitrogen clusters along with differences of the interaction energies. Therefore, we use its general results in order to discuss the structures of the mixed argon-nitrogen clusters. The phase diagram suggests that a phase separation in mixed cluster will occur, if the interactions of both the Ar-Ar and the N₂-N₂ pairs are strong. The lowest well depth of the N₂-N₂ potential (148.00 K for the T-shaped isomer) is close to that of the Ar-Ar potential (143.22 K), as outlined in Sec. II B. However, the average well depth of the N₂-N₂ pair is smaller than that of the Ar-Ar pair because of the anisotropic potential of the N₂-N₂ dimer due to the linear shape of nitrogen molecule.⁵⁵ Therefore, no phase separation is expected to occur in mixed Ar-N₂ clusters. Model C considers an isotropic core-shell structure, in which Ar atoms form a core, which is covered by N₂ molecules in an isotropic manner. In the calculated XPS spectrum, the intensity of the surface sites is smaller than that of the bulk sites. This intensity ratio is consistent with the experimental result. The intensity decrease of the Ar surface sites means that Ar atoms are covered by N₂ molecules. However, the difference in binding energy between the surface and bulk sites is only 0.075 eV. This energy difference is significantly smaller than that obtained from the experiments, where 0.23 eV are derived. Specifically, the Ar surface sites show a lower binding energy shift due to the induced polarization of the shell of N₂ molecules, which evidently does not occur in the experimental structures. In model D, we consider a partial core-shell structure, in which Ar atoms form the core, and N₂ molecules partially cover this core. The calculated spectrum shows that the number of Ar atoms occurring at surface sites is 11, and that of bulk sites is 17. The composition ratio of surface and bulk sites is fully consistent with the experimental results. The difference in binding energy between the surface and bulk sites is 0.24 eV, which is also consistent with that obtained from the experiments. In the phase diagram proposed by Clarke *et al.*,²¹ the partial core-shell structure is dominant when the Ar-N₂ potential is close to the N₂-N₂ potential, and the interactions of both the Ar-N₂ and N₂-N₂ potentials are smaller than that of the Ar-Ar potential. In fact, the well depth of the Ar-N₂ potential (160.91 K) is close to that of the N₂-N₂ potential (148.00 K for the T-shaped isomer). Both, the Ar-N₂ and N₂-N₂ potentials are anisotropic, and the average well depths of these potentials are smaller than that of the isotropic Ar-Ar potential. These potentials are favorable to yield partial core-shell structure, as proposed by the phase diagram.

These results clearly confirm that the Ar₂₈(N₂)₄₈ cluster (37% Ar) shows a partial core-shell structure, in which Ar atoms occupy the bulk sites and are partially covered by N₂ molecules.

The total energies of models B, C, and D relative to that of model A in the Ar₂₈(N₂)₄₈ cluster (37% Ar) are 0.07 eV, -0.20 eV, and -0.12 eV, respectively. The isotropic core-shell structure (model C) shows the lowest total energy, and the partial core-shell structure (model D) is the second lowest one. Due to the stronger Ar-Ar interactions relative to the Ar-N₂ and N₂-N₂ interactions, argon tends to form the core of mixed clusters, which is consistent with the earlier work.⁴¹ Furthermore, it becomes clear that the lowest energy structures are not always formed in jet expansions, which is also consistent with earlier studies on van der Waals clusters.⁴ The difference in total energy between models C and D is evidently too small (0.08 eV) to confine the mixed clusters in a unique lowest energy structure, so that reliable structure models simulating the experimental spectra cannot be based exclusively on a simple stability consideration. The partial core-shell structure also has the advantage regarding entropic effects, since the entropy of a partial core-shell structure is larger than that of an isotropic core-shell structure.

As described above, the present results suggest that the Ar₂₈(N₂)₄₈ cluster (37% Ar) shows the partial core-shell structure. We have also investigated whether the mixed Ar-N₂ clusters at high Ar contents show the partial core-shell structures, or not. Figure 3 shows the calculated Ar 2p_{3/2} XPS spectra for the mixed Ar-N₂ clusters with different compositions. The binding energy shifts and the intensities of

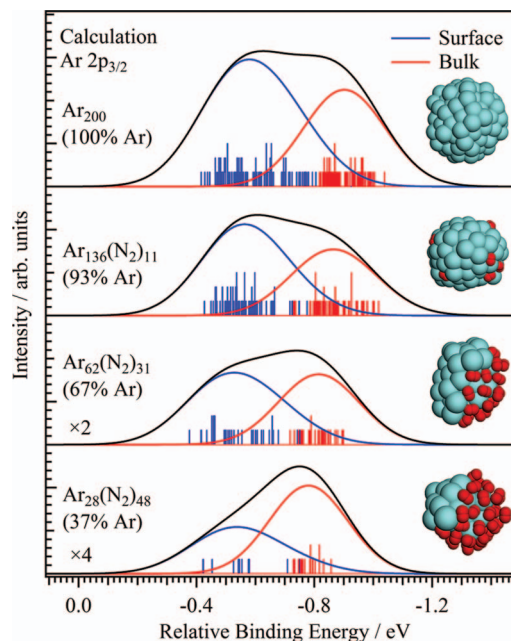


FIG. 3. Calculated Ar 2p_{3/2} binding energies (relative to the atomic values) and intensities of the surface and bulk sites in mixed Ar-N₂ clusters of different compositions, in comparison with the Ar₂₀₀ cluster. Simulated model structures of the mixed clusters are shown, in which Ar and N atoms are indicated by green and red spheres, respectively. Each vertical bar corresponds to the core level shift of different Ar sites in clusters. These are broadened by Gaussian line shapes (see text for further details).

the surface and bulk sites in the mixed Ar-N₂ clusters are indicated in Table I. The intensity of the argon surface sites is smaller than that of the bulk sites in Ar₂₈(N₂)₄₈ clusters (37% Ar). In Ar₆₂(N₂)₃₁ clusters (67% Ar), the intensity of the argon surface sites increases, where the number of Ar atoms on the surface and at bulk sites are found to be 34 and 28, respectively. The intensity ratio is consistent with the experimental results, in which the number of Ar atoms at surface and bulk sites is 32 and 30, respectively. The difference in binding energy between the surface and bulk site is 0.29 eV, which is close to the experimental value (0.27 eV). The Ar₁₃₆(N₂)₁₁ clusters (93% Ar) mainly consist of Ar atoms, and the calculated spectrum is close to that of homogeneous Ar cluster. The number of Ar atoms at surface and bulk sites is 80 and 56, respectively. These numbers are also in full agreement with the experimental results, where the number of Ar atoms at surface and bulk sites corresponds to 79 and 57, respectively. As a result, the mixed Ar-N₂ clusters show the partial core-shell structures irrespective of their composition.

IV. CONCLUSION

The structures of mixed Ar-N₂ clusters of different compositions were investigated by XPS spectra in the Ar 2*p*_{3/2} regime. The mixed Ar-N₂ clusters were formed in a supersonic jet expansion of the pre-mixed gases. The composition of Ar atoms in these mixed clusters was estimated from the Ar 2*p*_{3/2} XPS intensities by using neat Ar₂₀₀ clusters as a reference. The average number of N₂ molecules in mixed clusters is obtained from the previously published work on the cluster formation of nitrogen clusters in jet expansions,^{24,47,48,51} where the partial stagnation pressure of nitrogen in the gas mixture is used for this estimate. As a result, the compositions of the mixed Ar-N₂ clusters produced from the 10, 20, and 40 at. % Ar mixtures are evaluated to consist of Ar₂₈(N₂)₄₈ (37% Ar), Ar₆₂(N₂)₃₁ (67% Ar), and Ar₁₃₆(N₂)₁₁ (97% Ar), respectively.

The Ar 2*p*_{3/2} XPS spectrum for the Ar₂₈(N₂)₄₈ clusters (37% Ar) shows that the intensity of the Ar surface sites is smaller than that of the Ar bulk sites. This result suggests that Ar atoms are covered by N₂ molecules in the mixed clusters. We simulated the spectra for the several model structures of the mixed Ar-N₂ clusters, and compared those with the experimental results. This suggests that the Ar₂₈(N₂)₄₈ clusters (37% Ar) show a partial core-shell structure, in which Ar atoms form a core and are partially covered by N₂ molecules. Note that the proposed structure still remains somewhat ambiguous, due to the low signal strength of the XPS spectra, since we focused in the present work only on small sizes of mixed Ar-N₂ clusters. We also found that the mixed Ar-N₂ clusters of different compositions also show similar partial core-shell structures. These results are also rationalized in terms of the strength of anisotropy of inter-molecular interactions of the components bound in mixed clusters, where XPS is shown to be a sensitive and element-selective probe to study the internal structure of mixed clusters via binding energy shifts and the intensities of surface and bulk sites.

ACKNOWLEDGMENTS

Part of this work is supported by the Japan Society for the Promotion of Science (JSPS) Grant-in-Aids for Scientific Research (Nos. 19850029 and 20350014). Financial support by Deutsche Forschungsgemeinschaft (DFG) (Grant No. RU 420/8-1) is gratefully acknowledged. The authors would like to acknowledge kind support by the staff members of the UVSOR-II facility.

- ¹*Clusters of Atoms and Molecules*, edited by H. Haberland (Springer, Berlin, 1994).
- ²E. Rühl, *Int. J. Mass Spectrom.* **229**, 117 (2003).
- ³M. Tchapyguine, R. R. Marinho, M. Gisselbrecht, J. Schulz, N. Mårtensson, S. L. Sorensen, A. N. de Brito, R. Feifel, G. Öhrwall, M. Lundwall, S. Svensson, and O. Björneholm, *J. Chem. Phys.* **120**, 345 (2004).
- ⁴S. Kakar, O. Björneholm, J. Weigelt, A. R. B. de Castro, L. Tröger, R. Frahm, T. Möller, A. Knop, and E. Rühl, *Phys. Rev. Lett.* **78**, 1675 (1997).
- ⁵T. Hatsui, H. Setoyama, N. Kosugi, B. Wassermann, I. L. Bradeanu, and E. Rühl, *J. Chem. Phys.* **123**, 154304 (2005).
- ⁶G. J. Martyna and B. J. Berne, *J. Chem. Phys.* **90**, 3744 (1989).
- ⁷O. Björneholm, F. Federmann, F. Fössing, T. Möller, and P. Stampfli, *J. Chem. Phys.* **104**, 1846 (1996).
- ⁸A. Knop, B. Wassermann, and E. Rühl, *Phys. Rev. Lett.* **80**, 2302 (1998).
- ⁹M. Nagasaka, T. Hatsui, and N. Kosugi, *J. Electron Spectrosc. Relat. Phenom.* **166–167**, 16 (2008).
- ¹⁰M. Nagasaka, T. Hatsui, H. Setoyama, E. Rühl, and N. Kosugi, *J. Electron Spectrosc. Relat. Phenom.* **183**, 29 (2011).
- ¹¹T. Laarmann, K. von Haefen, H. Wabnitz, and T. Möller, *J. Chem. Phys.* **118**, 3043 (2003).
- ¹²A. Kanaev, L. Miseur, F. Edery, T. Laarmann, and T. Möller, *Phys. Rev. B* **69**, 125343 (2004).
- ¹³A. Lindblad, H. Bergersen, T. Rander, M. Lundwall, G. Öhrwall, M. Tchapyguine, S. Svensson, and O. Björneholm, *Phys. Chem. Chem. Phys.* **8**, 1899 (2006).
- ¹⁴M. Lundwall, A. Lindblad, H. Bergersen, T. Rander, G. Öhrwall, M. Tchapyguine, S. Svensson, and O. Björneholm, *J. Chem. Phys.* **125**, 014305 (2006).
- ¹⁵M. Lundwall, M. Tchapyguine, G. Öhrwall, R. Feifel, A. Lindblad, A. Lindgren, S. Sörensen, S. Svensson, and O. Björneholm, *Chem. Phys. Lett.* **392**, 433 (2004).
- ¹⁶M. Tchapyguine, M. Lundwall, M. Gisselbrecht, G. Öhrwall, R. Feifel, S. Sorensen, S. Svensson, N. Mårtensson, and O. Björneholm, *Phys. Rev. A* **69**, 031201 (2004).
- ¹⁷M. Lundwall, H. Bergersen, A. Lindblad, G. Öhrwall, M. Tchapyguine, S. Svensson, and O. Björneholm, *Phys. Rev. A* **74**, 043206 (2006).
- ¹⁸M. Lundwall, W. Pokapanich, H. Bergersen, A. Lindblad, T. Rander, G. Öhrwall, M. Tchapyguine, S. Barth, U. Hergenhan, S. Svensson, and O. Björneholm, *J. Chem. Phys.* **126**, 214706 (2007).
- ¹⁹K. Nagaya, H. Murakami, H. Iwayama, and M. Yao, *J. Electron Spectrosc. Relat. Phenom.* **166–167**, 11 (2008).
- ²⁰M. Nagasaka, N. Kosugi, and E. Rühl, *J. Chem. Phys.* **136**, 234312 (2012).
- ²¹A. S. Clarke, R. Kapral, and G. N. Patey, *J. Chem. Phys.* **101**, 2432 (1994).
- ²²F. Calvo and E. Yurtsever, *Phys. Rev. B* **70**, 045423 (2004).
- ²³R. G. Keesee, K. Kilgore, J. J. Breen, and A. W. Castleman, *Aerosol Sci. Technol.* **6**, 71 (1987).
- ²⁴A. A. Vostrikov and D. Y. Dubov, *Z. Phys. D* **20**, 429 (1991).
- ²⁵V. Molinero, D. Laria, and R. Kapral, *J. Chem. Phys.* **109**, 6844 (1998).
- ²⁶E. Fort, B. Lescop, A. de Martino, H. Vach, M. Châtelet, and F. Pradère, *Eur. Phys. J. D* **15**, 331 (2001).
- ²⁷S. Ishiuchi, M. Sakai, K. Daigoku, K. Hashimoto, and M. Fujii, *J. Chem. Phys.* **127**, 234304 (2007).
- ²⁸A. Takeda, H. S. Andrei, M. Miyazaki, S. Ishiuchi, M. Sakai, M. Fujii, and O. Dopfer, *Chem. Phys. Lett.* **443**, 227 (2007).
- ²⁹R. Signorell and M. Jetzki, *Faraday Discuss.* **137**, 51 (2008).
- ³⁰M. Miyazaki, A. Takeda, S. Ishiuchi, M. Sakai, O. Dopfer, and M. Fujii, *Phys. Chem. Chem. Phys.* **13**, 2744 (2011).

- ³¹M. Winkler, J. Harnes, and K. J. Børve, *J. Phys. Chem. A* **115**, 13259 (2011).
- ³²M. A. Kmetic and R. J. LeRoy, *J. Chem. Phys.* **95**, 6271 (1991).
- ³³S. Goyal, D. L. Schutt, and G. Scoles, *J. Chem. Phys.* **102**, 2302 (1995).
- ³⁴J. F. Winkel, C. A. Woodward, A. B. Jones, and A. J. Stace, *J. Chem. Phys.* **103**, 5177 (1995).
- ³⁵S. R. Atrill and A. J. Stace, *Phys. Chem. Chem. Phys.* **2**, 823 (2000).
- ³⁶A. Lindblad, M. Winkler, M. Tchapyguine, G. Öhrwall, S. Svensson, and O. Björneholm, *Surf. Sci.* **603**, 433 (2009).
- ³⁷J. W. Hewage and F. G. Amar, *J. Chem. Phys.* **119**, 9021 (2003).
- ³⁸J. W. Hewage, F. G. Amar, M.-F. de Feraudy, and G. Torchet, *Eur. Phys. J. D* **24**, 249 (2003).
- ³⁹G. Torchet, M.-F. de Feraudy, and Y. Loreaux, *J. Mol. Struct.* **485–486**, 261 (1999).
- ⁴⁰E. Fort, F. Pradère, A. De Martino, H. Vach, and M. Châtelet, *Eur. Phys. J. D* **1**, 79 (1998).
- ⁴¹E. Rühl, A. P. Hitchcock, P. Morin, and M. Lavollée, *J. Chim. Phys. Phys.-Chim. Biol.* **92**, 521 (1995).
- ⁴²T. Hatsui, E. Shigemasa, and N. Kosugi, *AIP Conf. Proc.* **705**, 921 (2004).
- ⁴³L. Pettersson, J. Nordgren, L. Selander, C. Nordling, K. Siegbahn, and H. Ågren, *J. Electron Spectrosc. Relat. Phenom.* **27**, 29 (1982).
- ⁴⁴M. P. Seah and W. A. Dench, *Surf. Interface Anal.* **1**, 2 (1979).
- ⁴⁵H. Zhang, D. Rolles, Z. D. Pešić, J. D. Bozek, and N. Berrah, *Phys. Rev. A* **78**, 063201 (2008).
- ⁴⁶M. Jurvansuu, A. Kivimäki, and S. Aksela, *Phys. Rev. A* **64**, 012502 (2001).
- ⁴⁷R. Flesch, A. A. Pavlychev, J. J. Neville, J. Blumberg, M. Kuhlmann, W. Tappe, F. Senf, O. Schwarzkopf, A. P. Hitchcock, and E. Rühl, *Phys. Rev. Lett.* **86**, 3767 (2001).
- ⁴⁸R. Flesch, N. Kosugi, I. L. Bradeanu, J. J. Neville, and E. Rühl, *J. Chem. Phys.* **121**, 8343 (2004).
- ⁴⁹R. Feifel, M. Tchapyguine, G. Öhrwall, M. Salonen, M. Lundwall, R. R. T. Marinho, M. Gisselbrecht, S. L. Sorensen, A. Naves de Brito, L. Karlsson, N. Mårtensson, S. Svensson, and O. Björneholm, *Eur. Phys. J. D* **30**, 343 (2004).
- ⁵⁰R. Karnbach, M. Joppien, J. Stapelfeldt, J. Wörmer, and T. Möller, *Rev. Sci. Instrum.* **64**, 2838 (1993).
- ⁵¹A. A. Vostrikov, D. Y. Dubov, and I. V. Samoilov, *Tech. Phys.* **39**, 1267 (1994).
- ⁵²J. Harnes, M. Winkler, A. Lindblad, L. J. Sæthre, and K. J. Børve, *J. Phys. Chem. A* **115**, 10408 (2011).
- ⁵³R. A. Aziz and H. H. Chen, *J. Chem. Phys.* **67**, 5719 (1977).
- ⁵⁴M. S. Bowers, K. T. Tang, and J. P. Toennies, *J. Chem. Phys.* **88**, 5465 (1988).
- ⁵⁵H.-J. Böhm and R. Ahlrichs, *Mol. Phys.* **55**, 1159 (1985).
- ⁵⁶N. Metropolis, A. W. Rosenbluth, M. N. Rosenbluth, A. H. Teller, and E. Teller, *J. Chem. Phys.* **21**, 1087 (1953).
- ⁵⁷M. Abu-Samha, K. J. Børve, L. J. Sæthre, G. Öhrwall, H. Bergersen, T. Rander, O. Björneholm, and M. Tchapyguine, *Phys. Chem. Chem. Phys.* **8**, 2473 (2006).
- ⁵⁸M. Abu-Samha, and K. J. Børve, *J. Chem. Phys.* **128**, 154710 (2008).
- ⁵⁹J. Harnes, M. Abu-samha, M. Winkler, H. Bergersen, L. J. Sæthre, and K. J. Børve, *J. Electron Spectrosc. Relat. Phenom.* **166–167**, 53 (2008).
- ⁶⁰T. M. Miller and B. Bederson, *Adv. At., Mol., Opt. Phys.* **13**, 1 (1978).
- ⁶¹J. O. Hirschfelder, C. F. Curtiss, and R. B. Bird, *The Molecular Theory of Gases and Liquids* (Wiley, New York, 1954).
- ⁶²R. E. Benfield, *J. Chem. Soc., Faraday Trans.* **88**, 1107 (1992).